Molecular Medicine

Antiinflammatory Activity of a Novel Folic Acid Targeted Conjugate of the mTOR Inhibitor Everolimus

Yingjuan Lu,[1] Nikki Parker,[1] Paul J Kleindl,[1] Vicky A Cross,[1] Kristin Wollak,[1] Elaine Westrick,[1] Torian W Stinnette,[1] Mark A Gehrke,[1†] Kevin Wang,[1] Hari Krishna R Santhapuram,[1] Fei You,[1] Spencer J Hahn,[1] Jeremy F Vaughn,[1] Patrick J Klein,[1] Iontcho R Vlahov,[1] Philip S Low,[2] and Christopher P Leamon[1]*

[1]Endocyte, Inc., West Lafayette, Indiana, United States of America; [2]Department of Chemistry, Purdue University, West Lafayette, Indiana, United States of America; *current address: Eli Lilly & Co., Indianapolis, Indiana, United States of America; and [†]current address: Upsher-Smith Laboratories, Inc., Maple Grove, Minnesota, United States of America

Folate receptor (FR)-β has been identified as a promising target for antimacrophage and antiinflammatory therapies. In the present study, we investigated EC0565, a folic acid–derivative of everolimus, as a FR-specific inhibitor of the mammalian target of rapamycin (mTOR). Because of its amphiphilic nature, EC0565 was first evaluated for water solubility, critical micelle formation, stability in culture and FR-binding specificity. Using FR-expressing macrophages, the effect of EC0565 on mTOR signaling and cellular proliferation was studied. The pharmacokinetics, metabolism and bioavailability of EC0565 were studied in normal rats. The *in vivo* activity of EC0565 was assessed in rats with adjuvant arthritis, a "macrophage-rich" model with close resemblance to rheumatoid arthritis. EC0565 forms micellar aggregates in physiological buffers and demonstrates good water solubility as well as strong multivalent FR-binding capacity. EC0565 inhibited mTOR signaling in rat macrophages at nanomolar concentrations and induced G0/G1 cell cycle arrest in serum-starved RAW264.7 cells. Subcutaneously administered EC0565 in rats displayed good bioavailability and a relatively long half-life (~12 h). When given at 250 nmol/kg, EC0565 selectively inhibited proliferating cell nuclear antigen expression in thioglycollate-stimulated rat peritoneal cells. With limited dosing regimens, the antiarthritic activity of EC0565 was found superior to that of etanercept, everolimus and a nontargeted everolimus analog. The *in vivo* activity of EC0565 was also comparable to that of a folate-targeted aminopterin. Folate-targeted mTOR inhibition may be an effective way of suppressing activated macrophages in sites of inflammation, especially in nutrient-deprived conditions, such as in the arthritic joints. Further investigation and improvement upon the physical and biochemical properties of EC0565 are warranted.

Online address: http://www.molmed.org
doi: 10.2119/molmed.2015.00040

INTRODUCTION

The current treatment paradigm in rheumatoid arthritis (RA) is more aggressive because of the necessity to initiate disease-modifying antirheumatic drugs (DMARDs) early to slow down disease progression (1). Among the nonbiologic DMARDs, methotrexate (MTX) has the longest duration of prescription use because of its effectiveness and affordability. Still, between 30 and 40% of RA patients do not experience remission while on MTX therapy, even when treated with a maximum tolerated dosing regimen (25–40 mg/wk) (2). In this patient population, biologic DMARDs have been used successfully to block proinflammatory cytokines, T-cell costimulatory molecules and autoreactive B cells (1). Nevertheless, injectable biologics are expensive and not suited for everyone because of increased risk of general infection, tuberculosis and malignancy (3). In addition, biologics are not specifically targeted to sites of inflammation and should not be used in combination because of the risk of systemic immunosuppression. Thus, nonbiologic DMARDs with mechanisms of action different from that of MTX are highly desirable, especially for compounds that specifically target inflammatory cells of interest.

In the fields of immunology and rheumatology, macrophage activation is a well-known phenomenon that contributes to the development and homeostasis of biological systems in response to a variety of cytokines, growth factors and

Address correspondence to *Christopher P Leamon, Endocyte, Inc., 3000 Kent Avenue, West Lafayette, IN 47906. Phone: 765-463-7175; Fax: 765-463-9271; E-mail: chrisleamon@endocyte.com.*
Submitted February 23, 2015; Accepted for publication July 8, 2015; Published Online (www.molmed.org) July 8, 2015.

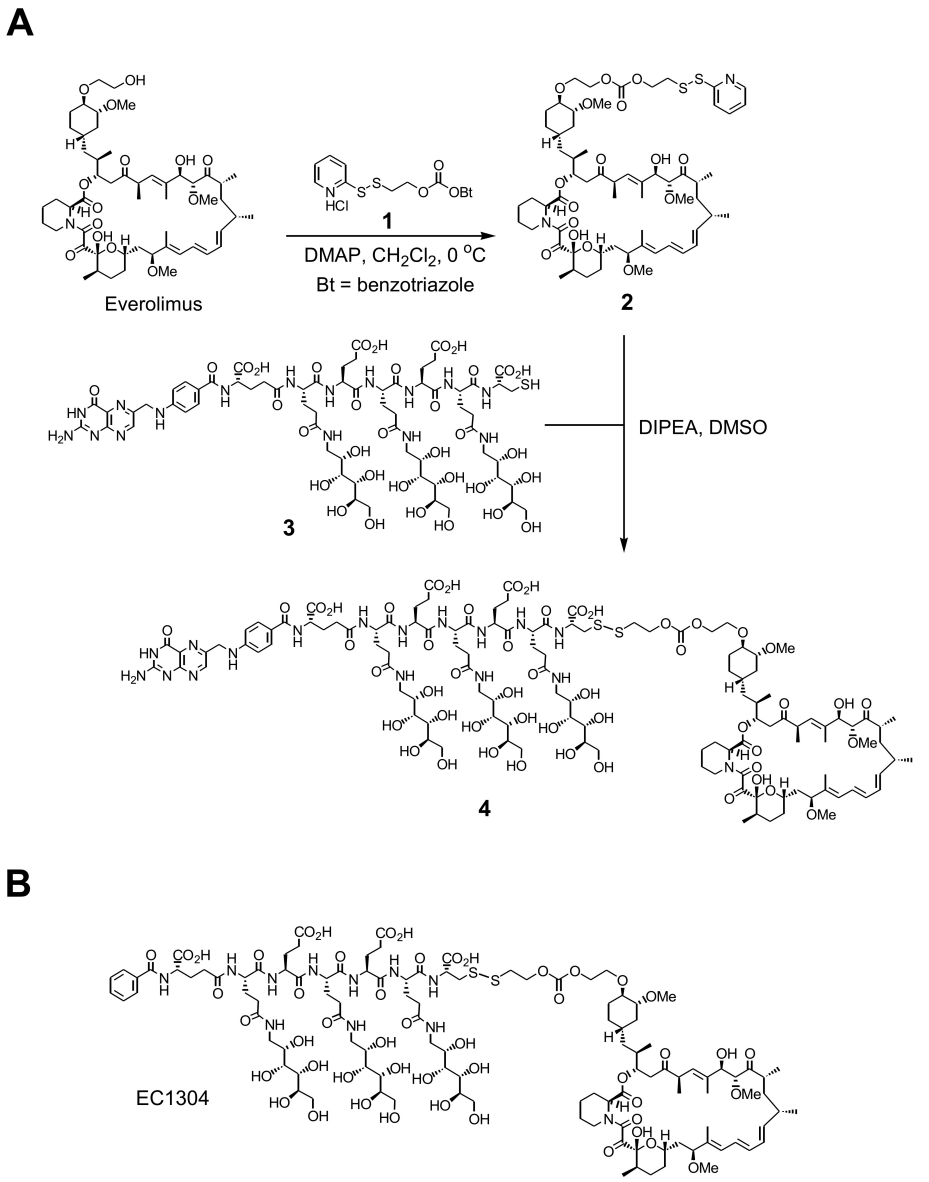

Figure 1. Chemical structures. (A) Everolimus, EC0565 (4) and its synthetic scheme (see Materials and Methods for details). (B) EC1304, a nontargeted EC0565 analog missing the FR-binding pteridyl amine moiety.

pathogens (4). Uncontrolled macrophage activation, however, is harmful and has been linked to the pathogenesis and progression of many human diseases (4). While activated macrophages have been broadly classified as M1 and M2, or proinflammatory "classical" and antiinflammatory "alternative" subsets, respectively, they exhibit high diversity and plasticity with mixed phenotypes coexisting in the same microenvironment (5). The main source of inflammatory macrophages actually derives from blood monocytes, which in turn derive from myeloid progenitors in the bone marrow (4). This continuous supply of blood monocytes gives rise to both hope and challenges of treating diseases in which activated macrophages play a central role in chronic inflammation (6).

The folate receptor (FR) family includes three cysteine-rich glycosylphosphatidylinositol–anchored glycoproteins, namely FR-α, -β and -γ (7). So far, only the FR-α and FR-β isoforms have been conclusively shown to display receptor binding functionality, that is, the ability to bind/internalize physiological folates with high specificity (8). While FR-α is frequently overexpressed by cancer cells of epithelial origins (7,8), FR-β is mostly expressed in functional form by activated macrophages (and their monocyte precursors) during inflammatory episodes that can lead to irreversible tissue and joint damage (9,10). Thus, FR-β–expressing macrophages have emerged as a promising target for antibody- or ligand-mediated drug delivery to control local and systemic inflammation (11). In animal models, anti-FR-β immunotoxins (12–14), folate-hapten immunotherapy (15,16) and folate-targeted aminopterin therapy (17,18) were found effective in treating models of arthritis (15–17), autoimmune uveitis (18), autoimmune encephalomyelitis (18), experimental fibrosis (13) and atherosclerosis (14). In early clinical trials, ^{99m}Tc-EC20 (etarfolatide), a FR-specific radioimaging agent, was shown to preferentially accumulate in inflamed arthritic joints in patients with RA (19) and osteoarthritis (20). Using folic acid (FA) as the targeting ligand, drugs with suitable mechanisms of action may be delivered to activated macrophages in sites of inflammation and be internalized via the FR-mediated endocytosis (21).

The mammalian target of rapamycin (mTOR) is an evolutionary conserved serine threonine kinase that has an essential function in cellular metabolism, growth and survival (22). The rapamycin analog, everolimus (RAD-001, Afinitor®) (Figure 1A), inhibits the mTOR complex 1 (mTORC1), which contains the protein raptor and is activated in response to growth factors, nutrients and cellular energy status (22). Clinically, everolimus is an efficacious drug and has been approved by the U.S. Food and Drug Administration for the treatment of advanced cancers (kidney, breast, pancreatic neuroendocrine) and non-

cancerous tumors (subependymal giant cell astrocytoma) (23). Besides their antiproliferative activities, mTOR inhibitors have been shown to regulate immune cell differentiation, activation and function (24–26). Everolimus-eluting coronary stents and oral everolimus have a long history of clinical utility in solid-organ transplantation to prevent acute and chronic rejections (27). Moreover, everolimus was found to alleviate RA symptoms in patients who had an inadequate response to MTX (28) and to induce disease inactivity in severe uveitis patients who became nonresponsive to cyclosporine A (29). Structurally, everolimus is slightly more polar than rapamycin, but it still exhibits low water solubility (~1–10 μmol/L) and poor/variable oral bioavailability (30). Finally, everolimus needs careful management to reduce side effects such as stomatitis, hyperglycemia, rash, noninfectious pneumonitis and potential viral reactivation (31). Thus, site-specific targeting of TOR inhibitors directly to diseased cells of interest may offer an improved bioavailability, target specificity and therapeutic index. Pertinently, a folate-targeted rapamycin conjugate was found to specifically target organs of interest and alleviate disease symptoms in mice with polycystic kidney disease (32). In the present study, we synthesized EC0565, a water-soluble FA derivative of everolimus, and investigated its biochemical and biological properties *in vitro* and *in vivo*.

MATERIALS AND METHODS

Reagents

Everolimus (molecular weight [MW] 958) was purchased from Haorui Pharma-Chem. For *in vitro* tests, everolimus was dissolved in 100% dimethyl sulfoxide (DMSO) and diluted in culture medium containing ≤1% DMSO. For *in vivo* use, everolimus was formulated based on the route of administration. For oral dosing, everolimus was first suspended in Phosal 50G (Phospholipids GmbH) and stored at –20°C in small aliquots. On the day of use, the everolimus/Phosal 50G stock preparation was diluted with water to form a milky solution. For dosing intraperitoneally or subcutaneously, everolimus was formulated in physiological phosphate-buffered saline (PBS) (pH 7.4) that contains 4% ethanol, 5% PEG-20 (MW ~982) and 5% polysorbate-80. Etanercept was purchased from CVS Pharmacy. Three previously published folate conjugates were all prepared in house: EC17 (MW 872) [folate-γ-ethylenediamine-fluorescein (33)], EC0746 (MW 2,236) [folate-γGlu(glucamino)-Glu-Glu(glucamino)-Glu-Glu(glucamino)-Cys-SS-ethyloxocarbonyl-γ(hydrazido)aminopterin (34)], and EC0923 (MW 672) [folate-D-Asp-D-Asp (17)]. The cell proliferation XTT [2,3-bis(2-methoxy-4-nitro-5-sulfo-phenyl)-2H-tetrazolium-5-carboxanilide] assay kit was obtained from Roche Applied Science. Antibodies to phospho-S6 ribosomal protein (p-RPS6, rabbit) and proliferating cell nuclear antigen (PCNA) (clone PC10, mouse) were obtained from Cell Signaling Technologies. Horseradish peroxidase (HRP)-coupled anti-rabbit and anti-mouse secondary antibodies were obtained from Jackson Immunoresearch and Santa Cruz Biotechnology, respectively. Anti-β-actin antibody was obtained from Rockland Immunochemicals. Enhanced chemiluminescence reagents were obtained from Thermo Scientific. All other reagents and test kits were purchased from major suppliers.

Animals, Sources of Macrophages and Cell Culture

All animal care and use was performed according to National Institutes of Health guidelines and was in compliance with protocols approved by the Purdue Animal Use and Care Committee. Female Lewis rats (175–200 g) were purchased from Harlan Sprague Dawley and allowed to acclimate for 1 wk. Generally, rats were fed a folate-deficient diet (Harlan Teklad) for 9–10 d before arthritis induction. Rat adjuvant arthritis (AIA) was induced by intradermal inoculation (at the base of the tail) of 0.5 mg heat-killed Mycobacteria butyricum (BD Diagnostic Systems) in 100 μL light mineral oil (Sigma). During the course of disease development, rats were scored three times a week according to the previously established criteria (17). Each paw was graded with a score of 0–4, with a maximum possible score of 16 for each animal.

Unless otherwise specified, all cells were maintained in a folate-free RPMI-1640 medium (Gibco BRL) (FFRPMI) containing 10% heat-inactivated fetal calf serum (HIFCS) and antibiotics under a 5% CO_2 atmosphere. RAW264.7 cells is a murine macrophage-derived tumor cell line grown in folate-deficient medium (17). The arthritic macrophages (AIA-mac) were obtained from peritoneal lavage of arthritic rats at the peak of the disease (~18–22 d after induction). The thioglycollate (TG)-elicited macrophages (TG-mac) were harvested from rats intraperitoneally dosed with an aged TG medium. After a 2-h plastic adherence, the respective macrophage populations were ~90% pure based on CD11b/c expression, and ~70% of the CD11b/c cells expressed a functional FR (17).

Synthesis of EC0565

The synthetic scheme of EC0565 (Figure 1A, compound 4) has been presented in an American Chemical Society Fall 2010 meeting poster (35) and is depicted in Figure 1A. To make 2-pyrridyldisulfanylethyl carbonyl–activated everolimus (Figure 1A, compound 2), everolimus (70 mg, 0.077 mmol) was dissolved in dichloromethane (500 μL) and cooled to 0°C. To this solution was added an activated carbonate, (Figure 1A, compound 1) (36) (56 mg, two equivalents) and 4-(dimethylamino)pyridine (26.6 mg, three equivalents). The reaction was allowed to occur with constant stirring at 0°C for 30 min. After a quick TLC check (5% methanol in dichloromethane) that showed some starting material remaining, additional quantities of 1 (28 mg) and 4-(dimethylamino)pyridine (13.3 mg) were added. The reaction was then allowed to go on for an additional 30 min at 0°C. After this time, the reaction mixture was loaded

onto a SiO_2 column and purified with a gradient of 0–4% methanol in dichloromethane. Approximately 59 mg (~68% yield) of the 2-pyridyldisulfanylethyl carbonate (Figure 1A, compound 2) was recovered after concentration. To make EC0565, to a suspension of carbohydrate-based folate spacer (Figure 1A, compound 3) (37) (33 mg, 0.020 mmol) in DMSO (1 mL) was added *N,N*-diisopropylethylamine (70 μL, 20 equivalents), followed by 2 (29 mg, 0.026 mmol). The reaction was allowed to stir at room temperature for 1.5 h. The crude reaction mixture was loaded directly onto a preparative C18 high-performance liquid chromatography (HPLC) column (Waters Xterra, 19 × 300 mm column) and purified using mobile phase consisting of 2 mmol/L sodium phosphate buffer, pH 7, and acetonitrile (gradient from 0 to 50% acetonitrile over 30 min). A total of 29 mg of the active EC0565 ingredient with an analytical HPLC purity of ≥95% was recovered (~40% yield corrected for phosphate buffer salts). The EC0565 compound identity was confirmed by NMR spectroscopy and liquid chromatography–tandem mass spectrometry (LC/MS/MS) with a chemical formula of $C_{121}H_{183}N_{17}O_{50}S_2$ and a MW of 2,740.

EC1304 (MW 2,550) is an everolimus control compound structurally analogous to EC0565 except for the FR-binding pteridyl amine moiety (Figure 1B). It was synthesized by methods similar to those described above for EC0565. Briefly, a carbohydrate spacer, incorporating a benzoyl moiety at the N-terminus rather than the pteroyl moiety found in spacer (Figure 1A, compound 3), was first synthesized by using standard solid-phase peptide synthesis techniques. This new spacer was coupled with carbonate 2 and purified as described previously.

Characterization of EC0565 Solubility, Aggregation and Binding Affinity

EC0565 powder was dissolved in PBS by gentle horizontal agitation, and the final concentration was calibrated by using UV absorption at 350 nm for FA [molar extinction coefficient: 7000 (38)]. To determine the critical micelle concentration (CMC), EC0565 was serially diluted in PBS containing 7 μmol/L Hoechst 33342 dye in a 96-well black microtiter plate (Thermo Electron Corporation). Fluorescence was measured in a Fluoroskan II fluorometer with excitation of 355 ± 10 nm (2 nm slit width) and emission of 460 ± 80 nm (1 nm slit width). The readout was background subtracted and fitted into a formula in Prism (version 5, GraphPad) (39). To measure FR-binding affinity, EC0565 was directly competed against ^{3}H-FA for binding to KB cells (40). The relative affinity (r.a.) value was defined as the inverse molar ratio of compound required to displace 50% of ^{3}H-FA bound to the cells. To assess EC0565 binding avidity, a ^{3}H-FA displacement assay was performed on KB cells preexposed to 0, 30 and 100 nmol/L and 1 μmol/L EC0565 for 30 min at 37°C. Afterward, the cells prebound with EC0565 were washed two times with culture medium and one time with cold PBS and were chased with 1 μmol/L ^{3}H-FA for 30 min at 4°C. For comparison, KB cells prebound to FA or two high-affinity folate ligands (EC0746, EC0923) (17) were subjected to the same ^{3}H-FA displacement as described. The percent maximal binding was determined on the basis of the ratio of cell-associated radioactivity with and without ligand preexposure.

EC0565 Stability in Cell Culture

EC0565 was spiked into FFRPMI supplemented with 0 or 10% HIFCS at 30 nmol/L. At various time points (0 min, 30 min, 1 h, 1.5 h, 2 h and 4 h), samples were immediately diluted 1:2 with methanol and injected directly at high flow (0.5 mL/min) onto a series of Waters XBridge BEH 1.7 μm VanGuard Pre-column 2.1 × 1.5 mm columns separated by a divert valve to prevent matrix from entering the second column or the detector. The analytes were separated by using an acetonitrile buffer gradient (0.112% ammonium, pH 9.3) at 0.3 mL/min and detected by LC/MS/MS. After the analyte elution and detection, a high-flow high-acetonitrile wash of the first column was completed before the subsequent injection. Calibration standards and quality-control samples were made in the same sample matrices. Under these conditions, everolimus eluted at ~1.6 min with a detection limit of 0.075 nmol/L.

Cell Proliferation and Viability Assays

As specified in the text, the FR-specific activity of EC0565 *in vitro* was assessed with and without FA or other high-affinity folate competitors (EC0923, EC17) at 1000-fold molar excess. For XTT assays, RAW264.7 cells in 96-well plates were serum-starved for 24 h before exposure to vehicle (1% DMSO in serum-free FFRPMI) or 10-fold serial dilutions (0–1 μmol/L) of everolimus and EC0565 with or without EC0923. The drug-containing media were replaced 2 h later, and the cells were incubated in FFRPMI with 10% HIFCS for a total of 72 h. The cell viability was assessed by adding XTT following the manufacturer's instructions (Roche Applied Science). The results were expressed as percent absorbance (minus background) relative to untreated control in triplicates. For cell cycle and Western blot (PCNA) analyses, serum-starved RAW264.7 cells were treated for 2 h as described above and harvested 48 h later. The cell cycle distribution was assessed by intracellular flow cytometry by using propidium iodide staining and ModFit analysis of DNA content. Total cell lysates (10 μg) were subjected to sodium dodecyl sulfate–polyacrylamide gel electrophoresis (SDS-PAGE) and immunoblotting with the PCNA monoclonal antibody (1:2,000; Cell Signaling Technology) and detected with the HRP-conjugated anti-mouse secondary antibody (1:5,000; Santa Cruz Biotechnology).

For *ex vivo* analysis of EC0565 effect on PCNA expression in TG-mac, TG-dosed rats (d 0, intraperitoneally) were given thymidine (300 mg/mL, intraperitoneally) on d 3 to synchronize peritoneal cells at the G1/S border. On d 4, rats were intraperitoneally dosed with everolimus (250 nmol/kg) or EC0565 (250 nmol/kg) with or without a 500-fold

excess of EC0923 (125 μmol/kg). Peritoneal macrophages harvested on d 6 were immediately lysed, and 20 μg of the total cell lysates were subjected to Western blot analysis for PCNA levels.

Measurement of S6 Ribosomal Protein Phosphorylation

Rat macrophages (TG-mac, AIA-mac) were pretreated for 1 h at 37°C in six-well plates with vehicle (FFRPMI with 0% HIFCS), everolimus (10 and 100 nmol/L) and EC0565 (1, 10, 30 and 100 nmol/L) with or without excess FA (100 μmol/L). After a 6-h chase in FFRPMI with 10% HIFCS, the cells were scraped into FFRPMI and washed with PBS, and the cell pellets were lysed in 0.1 mL radioimmunoprecipitation assay buffer containing phosphatase inhibitor cocktails 1 and 2 (1:100, Sigma-Aldrich). Protein concentrations of cell lysates were determined by using the bicinchoninic acid method (Thermo Scientific), and 20 μg of the lysate was resolved on a 10% Tris-HCl gel by SDS-PAGE. Proteins were transferred onto a 0.2 μm nitrocellulose membrane that was blocked and then probed with the p-RPS6 antibody (1:1,000; Cell Signaling Technology). After incubation with an HRP-conjugated anti-rabbit secondary antibody (1:5,000; Jackson Immunoresearch), blots were exposed to a Supersignal West Pico Chemiluminescent Substrate (Thermo Scientific) for 5 min, and bands were detected by using a G:BOX Chemi HR 16 gel imaging system (Syngene). Blots were then stripped and reprobed with an anti-β-actin antibody (1:2,000; Rockland Immunochemicals) as a control for protein loading.

Bioavailability and Pharmacokinetics Studies

Female Lewis rats with a rounded tip jugular vein catheter (Harlan) were dosed subcutaneously or intravenously with EC0565 at 2 μmol/kg. Venous blood samples (~300 μL) were collected for up to 8 h (intravenously) or 12 h (subcutaneously) into tubes containing 50 μL of 1.7 mg/mL K3-EDTA and 0.35 mg/mL *N*-maleoyl-β-alanine (0.35 mg/mL) in liquid form. Plasma was obtained immediately by twice centrifugation (1,960*g*, 3 min) at 4°C and stored in polypropylene tubes at –80°C until analysis. Because of the poor HPLC response of EC0565 (≥1 μg/mL lower limit of quantification [LLOQ]), sample analysis was conducted for free everolimus and everolimus after dithiothreitol treatment to obtain a total EC0565 concentration in the plasma. A portion of the EC0565 dosing solution was used to prepare a calibration working standard from which plasma calibration standards were generated. Thus, EC0565 extracted from the plasma was chemically treated to cleave the disulfide bond to produce everolimus, which was then detected by LC\MS\MS. The chromatography was reproducible and consistent between spiked matrix and sample derived from the dosed animals (data not shown). The maximum drug concentration in plasma (Cmax), time to Cmax (Tmax) and area under the curve (AUC) from time zero to the time of last measurable concentration were obtained. The absolute bioavailability (*F*) of EC0565 was calculated by using the following formula: AUC (subcutaneously)/AUC (intravenously).

Treatment of Rat Adjuvant Arthritis

All treatments started 10 d after induction and lasted for 2 consecutive weeks at once-a-week (QW; Mondays), twice-a-week (BIW; Mondays and Thursdays) or thrice-a-week (TIW; Mondays, Wednesdays and Fridays) dosing frequencies. On the first day of treatment (d 0), AIA rats with matching arthritis scores were distributed evenly across the treatment groups (n = 5). EC0565 was subcutaneously dosed, and its antiarthritic activity was assessed in three different experimental setups. First, EC0565 (500 nmol/kg) was compared with oral everolimus (500 nmol/kg) on a TIW regimen, whereas etanercept (10 mg/kg) was subcutaneously dosed every 3 d over a 12-d span. Second, to determine the FR specificity of EC0565 *in vivo*, EC0565 (500 nmol/kg) was coadministered with or without a 500-fold molar excess of EC0923 (125 μmol/kg) on d 0, 3 and 7. Lastly, EC0565 (100–1,000 nmol/kg, BIW or SIW) was compared against subcutaneously dosed everolimus (1,000 nmol/kg, QW), EC1304 (1,000 nmol/kg, QW) and EC0746 (1,000 nmol/kg, QW). At the completion of each study (4 d after the last treatment), rats were euthanized and processed for total paw weights (cut at the hairline) and spleen weights. The percent increase in paw and spleen weights over that of healthy controls were calculated as measurements of local and systemic activity, respectively. The removed hind paws were immersion fixed in 10% buffered formalin and assessed for radiographic joint damage by using a prespecified numerical grading system (0–26) for each hind foot (17).

Histopathology and Immunochemistry Evaluations

When desired, the formalin-fixed hind paws were also submitted for semiquantitative histopathological analysis as well as immunohistochemistry against CD68/ED1 (AbD Serotec). All tissue preparation and staining was performed at HistoTox Labs, Inc. The processed animal tissues were examined microscopically by a board-certified veterinary pathologist, Alison Bendele, at Bolder BioPATH. To obtain histological scores, a numerical grading system for joint damage (0–20) was used for each hind foot, as described previously (17). For CD68 immunostaining, CD68-positive osteoclasts were counted in five 25 × 250 μm fields in areas of bone resorption within the five most severely affected joints in each ankle. Osteoclasts in normal bone marrow or at the growth plate were not counted. On the other hand, CD68-positive macrophages were counted in five 25 × 125 μm fields in the areas of most intense synovial inflammation (below the lining) within the joints. Macrophages in the skin or periarticular tissue, or in normal synovial lining, were not counted. In both cases, counts from 10 fields across both ankles were averaged to obtain a mean value for each animal.

Statistics

Statistical analyses were performed using the computer program GraphPad

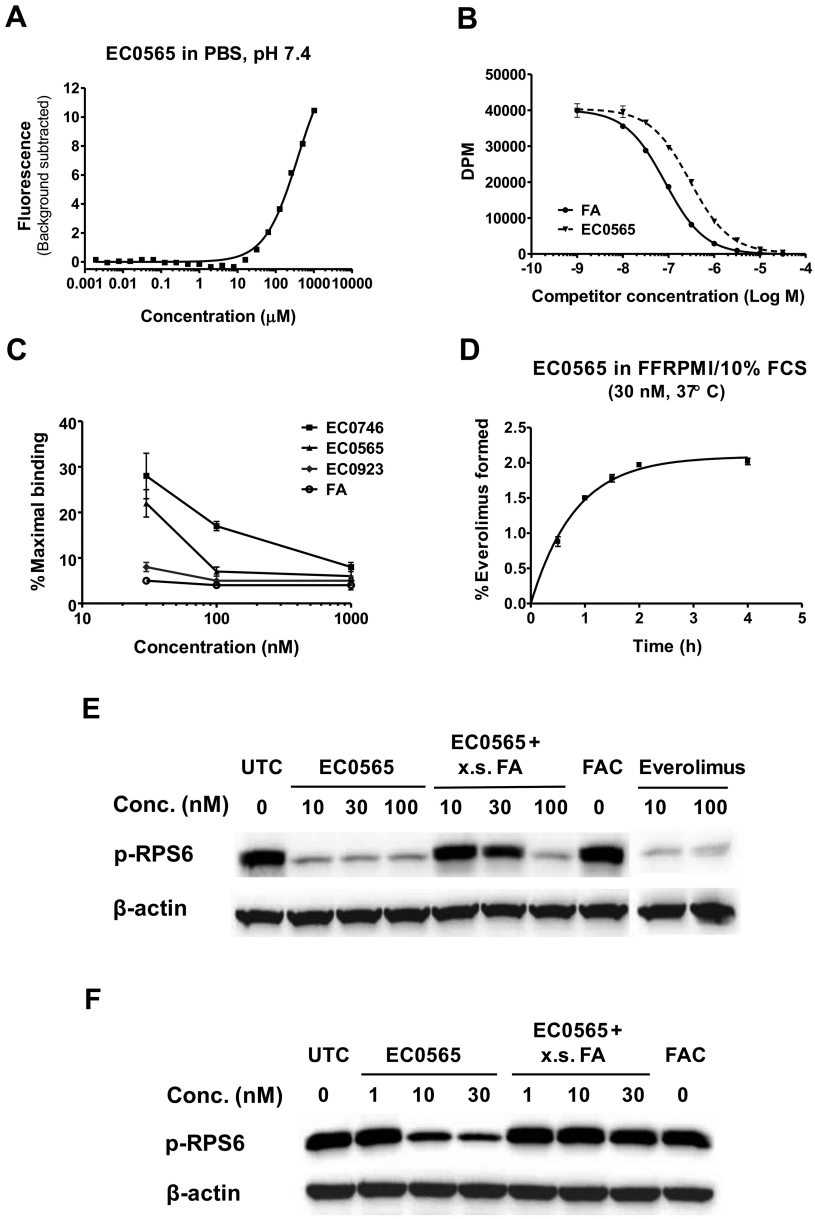

Figure 2. EC0565 characterization, stability and mTOR inhibition. (A) Fluorescence versus increasing EC0565/PBS concentration in a CMC assay. The R^2 values were >0.99. (B) Cell-associated radioactivity versus increasing concentrations of EC0565 and unlabeled FA in a ^{3}H-FA r.a. assay. The EC0565 r.a. value was determined to be ~0.28 (FA = 1). (C) ^{3}H-FA displacement on KB cells prebound with EC0565, FA or other high-affinity FR ligands (EC0746, r.a. ~0.5; EC0923, r.a. ~0.83). (D) Percent everolimus derived from 30 nmol/L EC0565 in FFRPMI with 0 or 10% HIFCS at 37°C for 4 h was detected by LC/MS/MS. (E, F) Western blot analysis of p-RPS6 in TG-mac (E) and AIA-mac (F) treated with EC0565 and everolimus at concentrations indicated. β-Actin was used as a loading control. FCS, fetal bovine serum; UTC, untreated control cells, FAC, folate acid alone control.

Prism (GraphPad Software Inc.). Data were analyzed by using a Student *t* test or Mann-Whitney *U* test (nonparametric). If applicable, data were further analyzed across treatment groups by using one-way analysis of variance (ANOVA). $^*P < 0.05$ was considered statistically significant in all tests (Figures 3 and 5–7).

RESULTS

EC0565 Biochemical and Biological Properties

The EC0565 construct (4) (Figure 1A) consists of (a) FA, the targeting ligand; (b) a saccharo–amino acid peptide-based spacer; (c) a disulfide/carbonate-containing linker; and (d) everolimus in the written sequence. Unlike everolimus (Figure 1A), which is practically insoluble in water, EC0565 was dissolved in PBS at >2 mmol/L (maximal solubility was not obtained). EC0565 in PBS was observed to "bubble up" easily on agitation and had a CMC value of ~2.2 μmol/L in a Hoechst 33342 dye assay (Figure 2A). Hoechst 33342 displays minimal fluorescence in hydrophilic environments but emits efficiently in hydrophobic surroundings (39). Further analysis by using a Zetasizer particle analyzer (Malvern) confirmed that the EC0565/PBS solution was polydispersed with different sizes of aggregates (data not shown). Furthermore, EC1304, the nontargeted amphiphilic everolimus control compound, also formed micellar aggregates in PBS with a CMC value of ~3.5 μmol/L (data not shown).

In a KB cell–based r.a. assay, EC0565 displayed a relatively high FR-binding affinity with an r.a. value of ~0.28, whereas FA was set at 1 (Figure 2B). In a reverse competitive assay (Figure 2C), KB cells were preexposed to 0–1 μmol/L FA, EC0565, or one of the two non-micelle–forming FA conjugates (EC0746, r.a. = 0.50; EC0923, r.a. = 0.84) (17). Upon chasing with 1 μmol/L ^{3}H-FA (see Materials and Methods), both FA and EC0923 remained cell-surface bound and were not displaced by ^{3}H-FA. At 30 nmol/L preexposure, EC0565 and EC0746 were partially displaced by ^{3}H-FA (~33-fold excess), likely due to their lower FR-binding affinities compared with ^{3}H-FA. At 100 nmol/L preexposure, EC0565 (with ~2× lower r.a. value than EC0746) bound stronger than EC0746 and was not displaced by ^{3}H-FA (~10-fold excess). This disparate result suggested that EC0565 in its polymeric/micellar form bound FRs with high avid-

ity, resulting in poor competition by the monomeric ^{3}H-FA ligands.

Because EC0565 has a bioreleasable linker susceptible to both reduction and potential hydrolysis (for example, carbonate moiety), we assessed the stability of EC0565 at 37°C in FFRPMI supplemented with 0 or 10% HIFCS (standard cell culture medium). After a 4-h incubation followed by LC/MS/MS quantitation, a maximal 2% everolimus was formed from 30 nmol/L EC0565 spiked into FFRPMI with 10% HIFCS (Figure 2D). The appearance of everolimus was serum-dependent because no observable everolimus peaks were seen in any EC0565 samples spiked into FFRPMI with 0% HIFCS. These results indicated that EC0565 remains relatively stable in aqueous solutions.

EC0565 Activity *In Vitro* and *Ex Vivo*

Inhibition of mTORC1 reduces phosphorylation of ribosomal protein S6 kinase (p-RPS6) via downregulation of p70S6 kinase, a major downstream effector (25). To measure EC0565 treatment response on p-RPS6, we used *ex vivo*–isolated TG-mac and AIA-mac that were previously shown to express an ~20-fold lower level of functional FR than that of RAW264.7 cells (21). Here, TG-mac (Figure 2E) and AIA-mac (Figure 2F) were treated with everolimus (10 and 100 nmol/L) or EC0565 (1, 10, 30 and 100 nmol/L) with or without excess FA. In both rat macrophages, EC0565 treatment resulted in a downregulation of p-RPS6 at nanomolar concentrations and appeared to be as active as everolimus on an equimolar basis. The inhibitory effect of EC0565 at ≤30 nmol/L could be partially blocked by 1,000-fold excess of FA. This result suggested that the amount of FRs on these rat macrophages were sufficiently high to mediate a FR-specific inhibition of the mTOR signaling pathway. Under normal cell culture conditions, EC0565 and everolimus did not exhibit any cytotoxic effect toward FR-expressing macrophages at ≤10 μmol/L (data not shown). However, in serum-starved (24-h) RAW264.7 cells, EC0565 was able to induce a dose-dependent cytostatic effect similar to that of everolimus (ED50: ~2 nmol/L, Figure 3A).

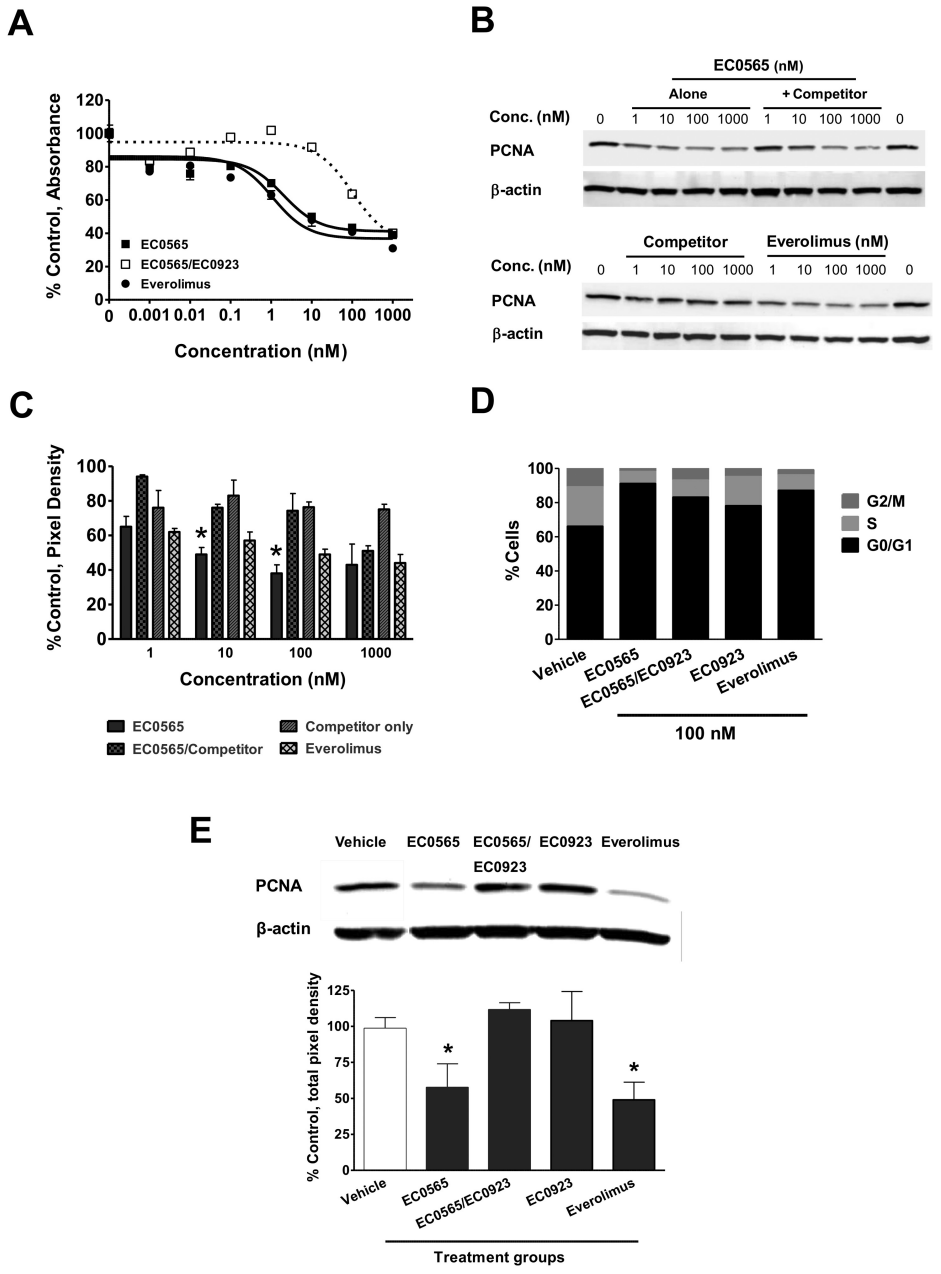

Figure 3. EC0565 antiproliferative activity. (A) Serum-starved RAW264.7 cells were exposed to EC0565 (with or without EC0923 as the competitor) or everolimus at a 10-fold serial increase in concentrations and assessed for cell viability by XTT. Western blot (B) and densitometric (C) analysis of PCNA expression in RAW264.7 cells treated with EC0565 (with or without EC17 as the competitor), the competitor alone or everolimus. (D) Cell cycle distribution in RAW264.7 cells treated with 100 nmol/L EC0565 (with or without EC0923 as the competitor), the competitor alone or everolimus. All folate competitors in A–D were used at 1,000-fold excess. (E) Representative Western blot and densitometric analysis of PCNA expression in TG-mac isolated from rats intraperitoneally dosed with EC0565 (250 nmol/kg), EC0565 plus 500-fold excess of EC0923, EC0923 alone or everolimus. The bars represent the mean ± standard error of the mean. *$P < 0.05$ in comparison to the vehicle control.

A

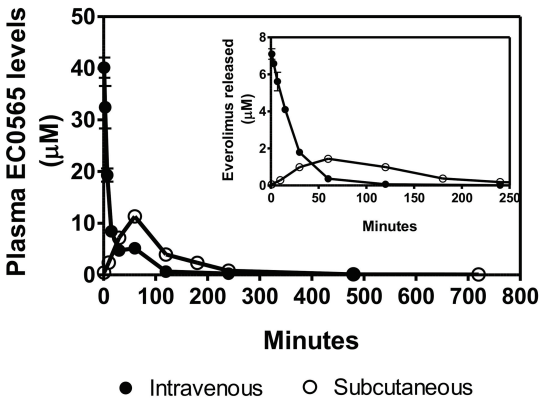

B

Dosing Route	Intravenous		Subcutaneous	
Plasma analytes	EC0565	Everolimus	EC0565	Everolimus
Cmax (μM)	45	7.8	9.9	1.4
Tmax (min)	-	-	60	60
t (1/2) (min)	155	180	722	104
AUC_{0-t} (nmol•min/mL)	845	181	1094	222
Total AUC_{0-t} (nmol•min/mL)	1026		1316	
Free drug released	17.6%		16.9	
Bioavailability (F)	-		128%	

Figure 4. Pharmacokinetics and bioavailability. Female Lewis rats (n = 3) with jugular vein catheters (Harlan) were given a single subcutaneous or intravenous injection of EC0565 at 2 μmol/kg. Plasma samples collected at various time points were analyzed by LC/MS/MS to quantitate EC0565 and everolimus levels. (A) The plasma concentration (μmol/L) as a function of time was plotted over 4 or 12 h postinjection for everolimus (insert) and EC0565, respectively. Values represent the mean ± standard deviation. (B) The table summarizes the values of PK analysis including Cmax, Tmax, $t_{½}$ (min), AUC_{0-t}, percentage of free drug (everolimus) released and bioavailability (*F*).

A 50-fold increase in the ED50 of EC0565 (~102 nmol/L) was observed in the presence of 1,000-fold excess of EC0923. Taken together, the FR specificity of EC0565 was concentration dependent: fully reversible at 1–10 nmol/L, partial reversible at 30–100 nmol/L and nonreversible at 1 μmol/L. Subsequent analysis also indicated that both everolimus and EC0565-treated RAW264.7 cells showed a dose-dependent reduction of PCNA expression (Figures 3B, C) and increased G0/G1 cell cycle arrest (Figure 3D). Likewise, EC0565 inhibition of PCNA expression and cell cycle arrest could be partially blocked by another unrelated folate competitor (EC17, folate-fluorescein [33]) with better competition seen at ≤10–100 nmol/L (Figure 3C).

Because rat macrophages do not proliferate in culture, we investigated the antiproliferative effect of EC0565 versus everolimus in TG-dosed rats after thymidine synchronization of peritoneal cells (see Materials and Methods). By Western blot analysis of PCNA expression in TG-mac harvested 2 d after a single intraperitoneal (IP) dose of everolimus (250 nmol/kg) and EC0565 (250 nmol/kg), a significantly decreased PCNA level was observed for both compounds (Figure 3E). Importantly, a 500-fold excess of intraperitoneally dosed EC0923 was also able to block the effect of EC0565 *in vivo*, whereas the competitor alone did not change PCNA levels in TG-mac.

Pharmacokinetics and Bioavailability

In rats, EC0565 administered intravenously or subcutaneously at 2 μmol/kg yielded a plasma Cmax value of ~45 μmol/L (1 min) and ~9.9 μmol/L (Tmax; 60 min), respectively (Figure 4A). The elimination half-life was ~4.7 times longer when EC0565 was dosed subcutaneously than intravenously at ~722 and 155 min, respectively (Figure 4B). The estimated bioavailability (*F*) of the subcutaneously dosed EC0565 was ~128% within an ~30% experimental error (data not shown). Owing to the releasable linker chemistry of EC0565 (4) (Figure 1A), free everolimus was detected in the plasma of EC0565-dosed animals regardless of the dosing route (Figure 4B). The plasma Cmax values of everolimus derived from intravenously or subcutaneously dosed EC0565 were ~7.8 μmol/L (1 min) and ~1.4 μmol/L (Tmax; 60 min), respectively (Figure 4B). On the basis of AUCs over the entire sampling period, the amounts of free everolimus released by EC0565 were similar for both administration routes (~17%). Taken together, it appeared that although EC0565 was completely bioavailable upon subcutaneously administration, it exhibited a much slower elimination profile in comparison to previous non-micelle–forming FA ligands (17,33).

EC0565 Antiarthritic Activity

EC0565 activity *in vivo* was assessed in AIA rats (Figure 5) by using previously established criteria (17). Starting 10 d after induction (denoted d 0), EC0565 (subcutaneously) and everolimus (oral dosing) were compared on a TIW equimolar basis (500 nmol/kg), whereas etanercept (subcutaneously) was dosed at 10 mg/kg every 3 d. Both oral everolimus and subcutaneously etanercept were found to alleviate AIA symptoms, such as increased arthritis score (Figure 5A), paw weight (Figure 5C) and

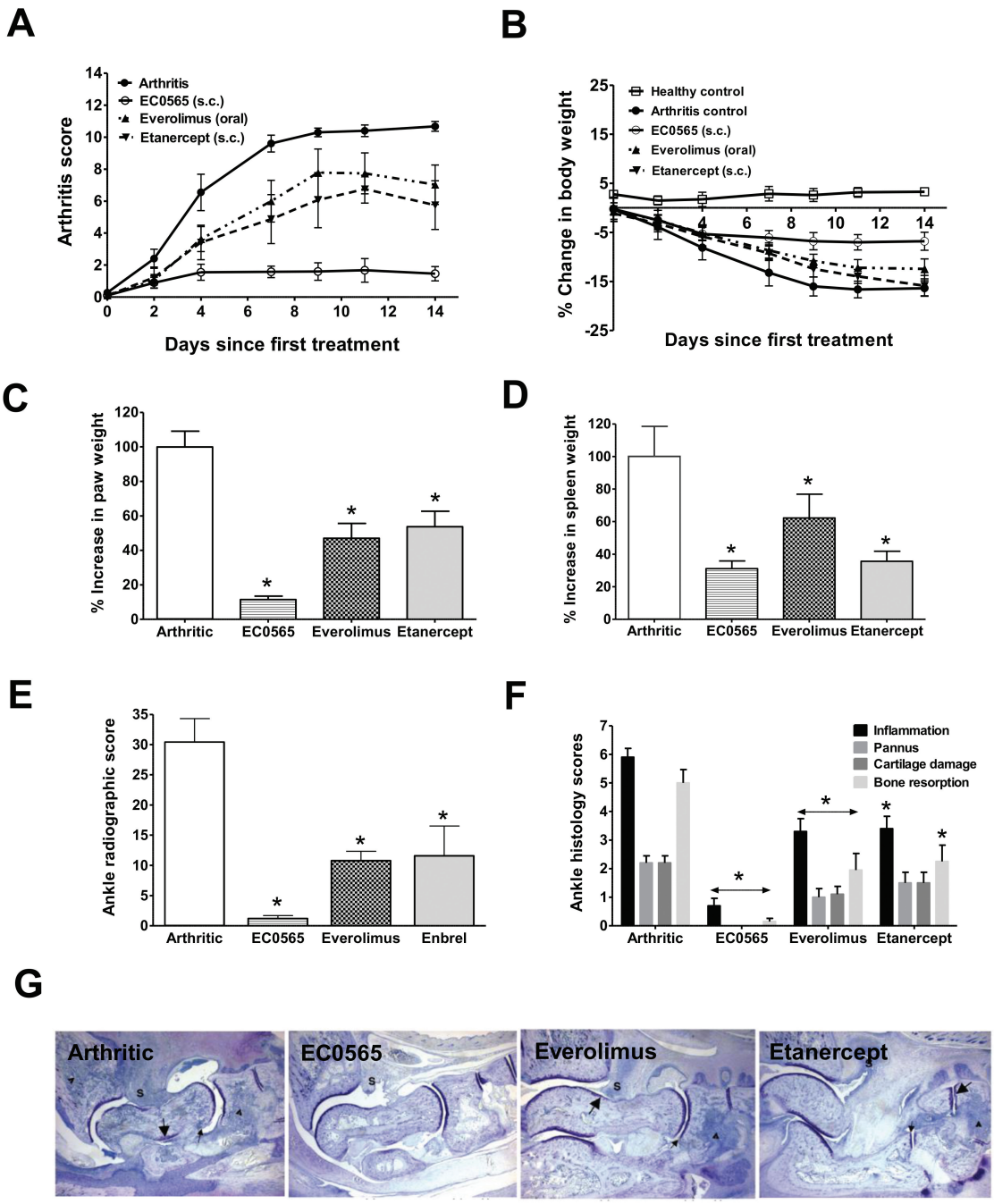

Figure 5. EC0565 antiarthritic activity. Rats with progressing AIA (n = 5) were given a TIW dosing regimen of EC0565 (subcutaneously) and everolimus (oral dose), both at 500 nmol/kg, and a 12-d span (every 3 d) of 10 mg/kg etanercept (subcutaneously) starting 10 d after induction. (A) Visual arthritis score plotted over days since first treatment. (B) Percent change in body weight. (C) Percent increase in paw weight. (D) Percent increase in spleen weight. (E) Radiographic score of arthritic hind paws. (F) Individual histological scores of ankle joints on a scale of 0–5 with a maximum of 20 per foot. (G) Representative photomicrographs (16×) of the ankle closest to the mean summed histological score. Significance was confirmed by ANOVA. *$P < 0.05$ when compared with the arthritic control group.

spleen weight (Figure 5D). However, EC0565 treatment was significantly more effective in all parameters assessed, and the animals maintained a healthy body weight (Figure 5B) during therapy. Radiographic analysis of the ankle joints confirmed significantly less bone and tissue damages in EC0565-treated animals than both of its comparators (Figure 5E). His-

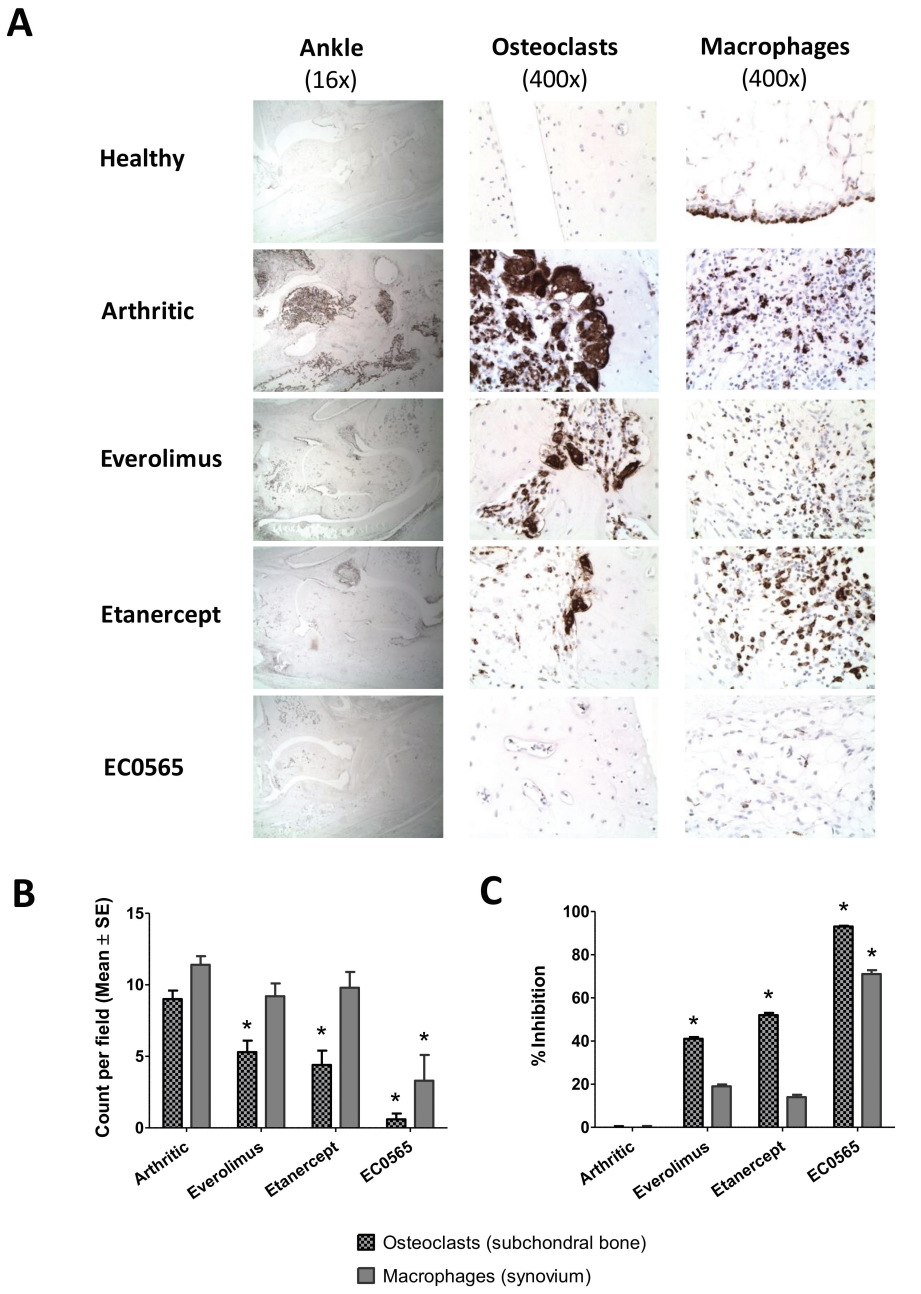

Figure 6. EC0565 effect on osteoclast and macrophage accumulation in arthritic joints. The ankle joint sections from AIA rats in Figure 5 were analyzed by immunohistochemistry for CD68. (A) Representative photomicrographs of CD68-stained ankle joint (16×), osteoclasts in subchondral bone (400×) and macrophages in the synovium (400×). (B) Counts per field averaged from the numbers of CD68-positive osteoclasts and macrophages in 10 fields across both ankles for each animal. (C) Percent inhibition calculated from the semiquantitated osteoclast and macrophage numbers for each group. *$P < 0.05$ when compared with the untreated control group by Student *t* test.

tologically (Figures 5F, G), animals treated with oral everolimus had significant reductions in all scored parameters (44–61%), whereas subcutaneously dosed etanercept yielded an ~42% reduction in inflammation and an ~55% reduction in bone resorption. Conversely, animals treated with EC0565 had significant (88–100%) decreases in the same assessed parameters. By using immunohistochemistry against CD68/ED1, a marker expressed by osteoclasts and macrophages, untreated arthritic control animals showed severe osteoclast-mediated bone resorption accompanied by a large influx of macrophages in the sublining layer of synovial tissues (Figure 6A, the second row). Healthy controls had no osteoclasts or macrophages in the same areas of interest (Figure 6A, the top row). Quantitatively, the diseased control animals had an average count of 9.0 ± 0.6 osteoclasts per field and 11.4 ± 0.6 macrophages per field (Figure 6B). Remarkably, EC0565 treatment (at disease onset) reduced osteoclast counts to less than one per field (Figure 6B). In all dosing groups analyzed (Figures 6B, C), osteoclast counts were significantly reduced by treatment with everolimus (~41%), etanercept (~53%) or EC0565 (~93%). Likewise, synovial macrophage counts were significantly reduced by treatment with EC0565 (~71%). Everolimus treatment reduced macrophage counts by ~19%, which was nearly significant ($P = 0.068$, Figure 6C). On the other hand, etanercept treatment did not yield a statistically significant reduction (~14%) of macrophage counts ($P = 0.242$, Figure 6C).

To evaluate FR specificity *in vivo*, we conducted competition studies in AIA rats by using EC0923 as the folate competitor for EC0565 (Figure 7). Here, EC0565 (500 nmol/kg) was subcutaneously dosed on d 0, 3 and 7 alone or in combination with a 500-fold molar excess of EC0923 (250 μmol/kg). Interestingly, EC0565 activity was only partially blocked by EC0923 on the basis of arthritis score (Figure 7A), paw weight (Figure 7B) and ankle radiographic analysis (Figure 7C). There was no difference in spleen weight in the EC0565-treated groups with or without the competitor (Figure 7D). Because EC0565 displays a long circulation half-life in the plasma (Figure 4B), EC0565 dose/frequency responses were then compared against

everolimus and EC1304, the nontargeted everolimus control compound (Figure 7E). EC0746, the highly effective and FR-specific folate-aminopterin conjugate (17), was also included in this study. All compounds were administered subcutaneously, and the efficacy comparison was performed based on percent inhibition in paw edema calculated from percent increase in paw weight over that of the arthritic control. As illustrated in Figure 7E, EC0565 demonstrated a dose-dependent antiarthritic activity that was more efficacious when dosed BIW than QW for 2 consecutive weeks. More importantly, subcutaneously infrequently (QW) dosed everolimus or EC1304 failed to produce any significant activity at 1,000 nmol/kg. Under the same treatment conditions, EC0565 was able to produce a significant inhibition (~71%) of paw edema, which was similar to that of our previously disclosed compound EC0746 (~82%).

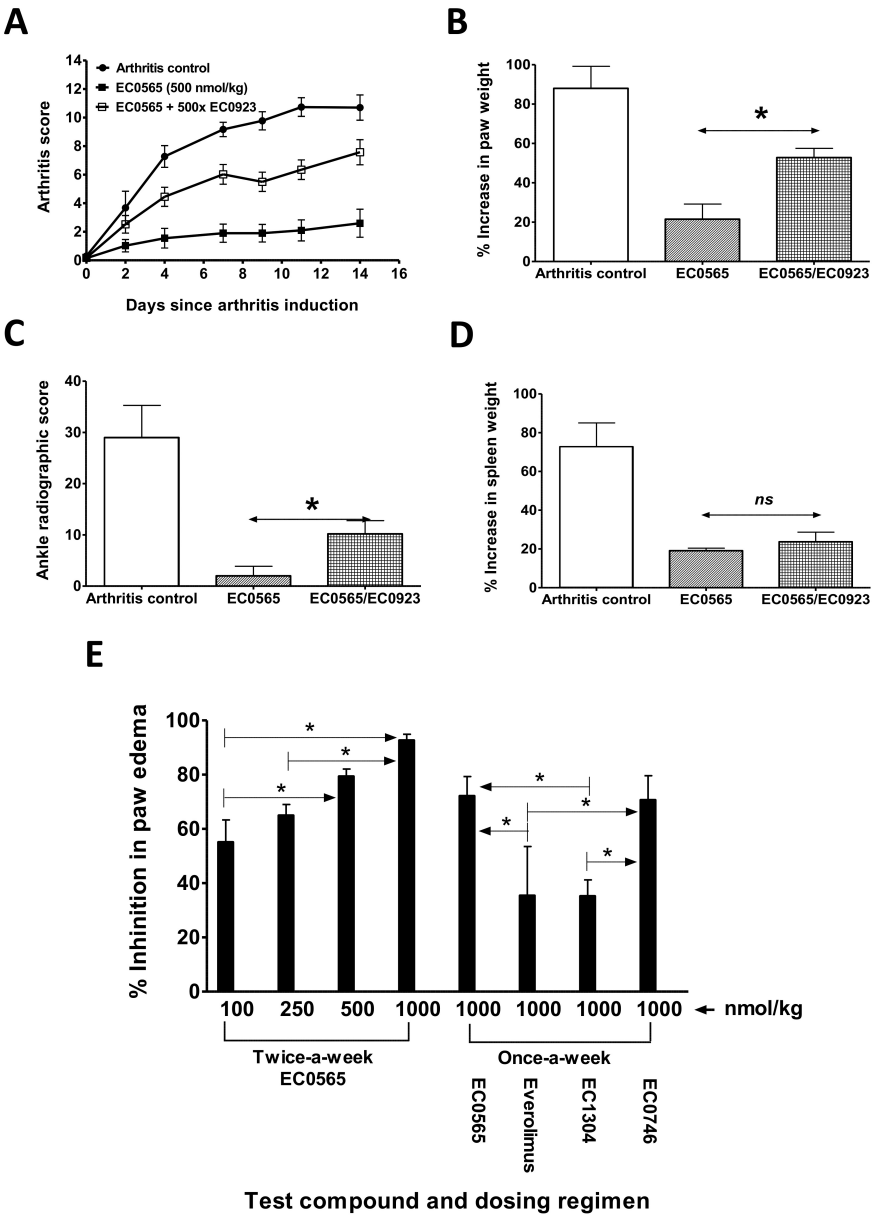

Figure 7. FR-specific activity of EC0565 *in vivo*. AIA rats (n = 5) were subcutaneously dosed on d 0, 3 and 7 with EC0565 (500 nmol/kg) with or without a 500-fold molar excess of EC0923 as the competitor (A–D). (A) Arthritis score. (B) Percent increase in paw weight. (C) Radiographic analysis of arthritic hind paws. (D) Percent increase in spleen weight. (E) EC0565 dosed at 100–1,000 nmol/kg (BIW or QW) were compared against subcutaneous everolimus (1,000 nmol/kg, QW), EC1304 (1,000 nmol/kg, QW) and EC0746 (1,000 nmol/kg, QW). Shown is the percent inhibition in paw edema calculated from the percent increase in paw weight for each treatment group over that of the arthritic control group. *$P < 0.05$ for the comparing groups, as indicated (ns = insignificant).

DISCUSSION

Despite the clinical success of mTOR inhibitors, we believe that the full therapeutic potential of these compounds has not yet been reached. The mTOR signaling pathway provides a direct metabolic link between immune cells and microenvironment, but the immunologic regulation due to mTOR inhibition is complex and cell type dependent (24,25). In monocytes and macrophages, mTORC1 inhibitors such as rapamycin and everolimus appear to evoke pro- and antiinflammatory cytokine production (25,41), macrophage polarization (42) and autophage (43). Targeting mTOR signaling pathway via FRs may be a useful approach to curtail autoimmune and other diseases caused or worsened by activated macrophages. Compared to everolimus, EC0565 displayed improved water solubility (~200- to 2,000-fold in PBS), complete bioavailability (subcutaneously) and FR-specific activities both *in vitro* and *in vivo*. Under serum-starved conditions, EC0565 induced G0/G1 cell cycle arrest at the PCNA level and dramatically hampered RAW264.7 cells' ability to proliferate (Figures 3A–D). In nonproliferating TG-mac and AIA-mac, EC0565 demonstrated a dose-dependent inhibition of mTORC1-dependent RPS6 phosphorylation (p-RPS6) (Figures 2E, F). Because of its self-aggregation and strong FR-binding affinity/avidity (Figures 2A–C), EC0565 competition was not

easily demonstrated with monomeric folate ligands but better competition was always seen at ≤100 nmol/L. Regardless of the study parameters, however, EC0565 activities *in vitro* could be blocked at least partially by a 1,000-fold excess of FA or other high-affinity folate competitors (EC0923, EC17). Moreover, EC0565 administered locally (intraperitoneally) to rats after TG activation showed a reduction in PCNA expression by the peritoneal cells, and the effect was fully blocked by EC0923 (Figure 3E). However, EC0565 was found less stable in the presence of serum (Figure 2D), and ~17% of free everolimus was detected in rat plasma after a single intravenous or subcutaneous administration (Figure 4B). The detection of free everolimus *in vivo* is likely due to EC0565 degradation in the blood, first-pass liver metabolism and/or degradation within the tissues. Thus, the lack of full competition of EC0565 *in vitro* and *in vivo* may be explained not only by its high FR-binding avidity (that is, not readily displaced by monomeric folate competitors), but also by the premature release of the parent drug. Interestingly, as shown in Figure 7E, EC0565 was found to be significantly more active than equimolar doses of everolimus and EC1304 (all dosed subcutaneously). This is important, since EC1304 was structurally similar to EC0565 and it had similar CMC values as EC0565. Finally, EC0565 appeared to be superior to both everolimus and etanercept when administered via their respective clinical dosing routes in this rat arthritis model (Figure 5). Immunohistochemically, EC0565 treatment (500 nmol/kg, subcutaneously) substantially and significantly reduced $CD68^+$ osteoclasts and macrophage counts in bone marrow and synovium of arthritic animals (Figures 6B, C). In comparison, treatment with everolimus (500 nmol/kg, oral dose) or etanercept (10 mg/kg, subcutaneously) significantly reduced osteoclasts counts, but had only mild effects on synovial macrophages. Although they were not directly quantified in this analysis, neutrophils were seen in considerably greater numbers than macrophages. For example, in the case of a field containing nine macrophages, ~40 neutrophils were observed (data not shown).

Taken together, these data suggest that the FR targeting component of EC0565 certainly contributed to the enhanced antimacrophage activity *in vitro* and *in vivo*. Interestingly, despite a completely different mechanism of action, EC0565 (everolimus; mTOR) and EC0746 (aminopterin; dihydrofolate reductase) were found to be similarly active in halting AIA progression with an ~71–82% inhibition in paw edema (Figure 7E). Because of the compound availability, the EC0565 maximum tolerated dose was not reached in female Lewis rats, but it was tested against subcutaneous everolimus at 0.52 μmol/kg (daily for 28 d). No treatment-related gross toxicity or histopathology changes were detected, with the exception of a reduced thymus weight similar to that of everolimus (data not shown).

CONCLUSION

As a small injectable molecule, the prolonged circulation half-life of EC0565 may be used in favor of an infrequent dosing regimen (for example, QW). However, EC0565 was challenging to synthesize and formulate because of its amphiphilic nature. Chemical modification and alternative formulations are being explored to improve upon EC0565 with regards to physical and biochemical properties, premature free drug release and FR specificity. Future work is also warranted to explore the utility of a folate-targeted mTOR inhibitor in other disease models. Our data suggest that a folate-targeted mTOR inhibitor may offer an alternative to biologics after MTX failure in RA or other disease indications.

DISCLOSURE

The authors declare that they have no competing interests as defined by *Molecular Medicine*, or other interests that might be perceived to influence the results and discussion reported in this paper.

REFERENCES

1. Singh JA, *et al.* (2012) 2012 update of the 2008 American College of Rheumatology recommendations for the use of disease-modifying antirheumatic drugs and biologic agents in the treatment of rheumatoid arthritis. *Arthritis Care Res. (Hoboken).* 64:625–39.
2. Halilova KI, *et al.* (2012) Markers of treatment response to methotrexate in rheumatoid arthritis: where do we stand? *Int. J. Rheumatol.* 2012:978396.
3. Khraishi M. (2009) Comparative overview of safety of the biologics in rheumatoid arthritis. *J. Rheumatol. Suppl.* 82:25–32.
4. Ginhoux F, Jung S. (2014) Monocytes and macrophages: developmental pathways and tissue homeostasis. *Nat. Rev. Immunol.* 14:392–404.
5. Martinez FO, Gordon S. (2014) The M1 and M2 paradigm of macrophage activation: time for reassessment. *F1000Prime Rep.* 6:13.
6. Davignon JL, *et al.* (2013) Targeting monocytes/macrophages in the treatment of rheumatoid arthritis. *Rheumatology (Oxford).* 52:590–8.
7. Chen C, *et al.* (2013) Structural basis for molecular recognition of folic acid by folate receptors. *Nature.* 500:486–9.
8. Wibowo AS, *et al.* (2013) Structures of human folate receptors reveal biological trafficking states and diversity in folate and antifolate recognition. *Proc. Natl. Acad. Sci. U. S. A.* 110:15180–8.
9. Tsuneyoshi Y, *et al.* (2012) Functional folate receptor beta-expressing macrophages in osteoarthritis synovium and their M1/M2 expression profiles. *Scand. J. Rheumatol.* 41:132–40.
10. Nakashima-Matsushita N, *et al.* (1999) Selective expression of folate receptor beta and its possible role in methotrexate transport in synovial macrophages from patients with rheumatoid arthritis. *Arthritis Rheum.* 42:1609–16.
11. Hansen M, Low P. (2011) Folate receptor positive macrophages: cellular targets for imaging and therapy of inflammatory and autoimmune diseases. In: *Targeted Drug Strategies for Cancer and Inflammation*. Jackman AL, Leamon CP (eds.) New York, Springer, pp. 181–93.
12. Nagai T, *et al.* (2006) In vitro and in vivo efficacy of a recombinant immunotoxin against folate receptor beta on the activation and proliferation of rheumatoid arthritis synovial cells. *Arthritis Rheum.* 54:3126–34.
13. Nagai T, *et al.* (2010) Effect of an immunotoxin to folate receptor beta on bleomycin-induced experimental pulmonary fibrosis. *Clin. Exp. Immunol.* 161:348–56.
14. Furusho Y, *et al.* (2012) Novel therapy for atherosclerosis using recombinant immunotoxin against folate receptor beta-expressing macrophages. *J. Am. Heart Assoc.* 1:e003079.
15. Yi YS, Ayala-Lopez W, Kularatne SA, Low PS. (2009) Folate-targeted hapten immunotherapy of adjuvant-induced arthritis: comparison of hapten potencies. *Mol. Pharm.* 6:1228–36.
16. Paulos CM, *et al.* (2006) Folate-targeted immunotherapy effectively treats established adjuvant

and collagen-induced arthritis. *Arthritis Res. Ther.* 8:R77.
17. Lu Y, *et al.* (2011) Treatment of experimental adjuvant arthritis with a novel folate receptor-targeted folic acid-aminopterin conjugate. *Arthritis Res. Ther.* 13:R56.
18. Lu Y, *et al.* (2014) Folate receptor-targeted aminopterin therapy is highly effective and specific in experimental models of autoimmune uveitis and autoimmune encephalomyelitis. *Clin. Immunol.* 150:64–77.
19. Matteson EL, *et al.* (2009) Assessment of disease activity in rheumatoid arthritis using a novel folate targeted radiopharmaceutical Folatescan. *Clin. Exp. Rheumatol.* 27:253–9.
20. Kraus VB, *et al.* (2013) Direct in vivo evidence of activated macrophages in human Osteoarthritis. *Osteo Cartilage.* 21(Suppl.):S42.
21. Lu Y, Leamon CP. (2011) Targeting activated macrophages via a functional folate receptor for potential treatment of autoimmune/inflammatory disorders. In: *Targeted Drug Strategies for Cancer and Inflammation.* Jackman AL, Leamon CP (eds.) New York, Springer, pp. 195–216.
22. Shimobayashi M, Hall MN. (2014) Making new contacts: the mTOR network in metabolism and signalling crosstalk. *Nat. Rev. Mol. Cell. Biol.* 15:155–62.
23. Porta C, Paglino C, Mosca A. (2014) Targeting PI3K/Akt/mTOR signaling in cancer. *Front. Oncol.* 4:64.
24. Powell JD, Pollizzi KN, Heikamp EB, Horton MR. (2012) Regulation of immune responses by mTOR. *Annu. Rev. Immunol.* 30:39–68.
25. Katholnig K, Linke M, Pham H, Hengstschlager M, Weichhart T. (2013) Immune responses of macrophages and dendritic cells regulated by mTOR signalling. *Biochem. Soc. Trans.* 41:927–33.
26. Narita M, *et al.* (2011) Spatial coupling of mTOR and autophagy augments secretory phenotypes. *Science.* 332:966–70.
27. Mabasa VH, Ensom MH. (2005) The role of therapeutic monitoring of everolimus in solid organ transplantation. *Ther. Drug Monit.* 27:666–76.
28. Bruyn GA, *et al.* (2008) Everolimus in patients with rheumatoid arthritis receiving concomitant methotrexate: a 3-month, double-blind, randomised, placebo-controlled, parallel-group, proof-of-concept study. *Ann. Rheum. Dis.* 67:1090–5.
29. Heiligenhaus A, *et al.* (2013) Everolimus for the treatment of uveitis refractory to cyclosporine A: a pilot study. *Graefes Arch. Clin. Exp. Ophthalmol.* 251:143–52.
30. Kirchner GI, Meier-Wiedenbach I, Manns MP. (2004) Clinical pharmacokinetics of everolimus. *Clin. Pharmacokinet.* 43:83–95.
31. Kaplan B, Qazi Y, Wellen JR. (2014) Strategies for the management of adverse events associated with mTOR inhibitors. *Transplant Rev. (Orlando).* 28:126–33.
32. Shillingford JM, Leamon CP, Vlahov IR, Weimbs T. (2012) Folate-conjugated rapamycin slows progression of polycystic kidney disease. *J. Am. Soc. Nephrol.* 23:1674–81.
33. Lu Y, Low PS. (2002) Folate targeting of haptens to cancer cell surfaces mediates immunotherapy of syngeneic murine tumors. *Cancer Immunol. Immunother.* 51:153–62.
34. Vlahov IR, *et al.* (2011) Design and regioselective synthesis of a new generation of targeted therapeutics. Part 3: Folate conjugates of aminopterin hydrazide for the treatment of inflammation. *Bioorg. Med. Chem. Lett.* 21:1202–5.
35. Vlahov IR, *et al.* (2010) Design and synthesis of folate conjugates of rapamycin and everolimus. Presented at: 240th ACS National Meeting; 2010 Aug 22–26; Boston, MA.
36. Vlahov IR, *et al.* (2006) Design and regioselective synthesis of a new generation of targeted chemotherapeutics. Part 1: EC145, a folic acid conjugate of desacetylvinblastine monohydrazide. *Bioorg. Med. Chem. Lett.* 16:5093–6.
37. Vlahov IR, *et al.* (2010) Carbohydrate-based synthetic approach to control toxicity profiles of folate-drug conjugates. *J. Org. Chem.* 75:3685–91.
38. Temple CJ, Montgomery JA. (1984) Chemistry and biochemistry of folates. In: *Folates and Pterins.* Blakley RL, Benkovic SJ (eds.) New York, John Wiley & Sons, pp. 61.
39. Jumpertz T, *et al.* (2011) High-throughput evaluation of the critical micelle concentration of detergents. *Anal. Biochem.* 408:64–70.
40. Leamon CP, You F, Santhapuram HK, Fan M, Vlahov IR. (2009) Properties influencing the relative binding affinity of pteroate derivatives and drug conjugates thereof to the folate receptor. *Pharm. Res.* 26:1315–23.
41. Xie S, *et al.* (2014) Identification of a role for the PI3K/AKT/mTOR signaling pathway in innate immune cells. *PLoS One.* 9:e94496.
42. Byles V, *et al.* (2013) The TSC-mTOR pathway regulates macrophage polarization. *Nat. Commun.* 4:2834.
43. Sergin I, Razani B. (2014) Self-eating in the plaque: what macrophage autophagy reveals about atherosclerosis. *Trends Endocrinol. Metab.* 25:225–34.
44. Oerlemans C, *et al.* (2011) A novel approach to identify non-palpable breast lesions combining fluorescent liposomes and magnetic resonance-guided high intensity focused ultrasound-triggered release. *Eur. J. Pharm. Biopharm.* 77:458–64.

Cite this article as: Lu Y, *et al*. (2015) Antiinflammatory activity of a novel folic acid targeted conjugate of the mTOR inhibitor everolimus. *Mol. Med*. 21:584–96.